International Immunopharmacology 77 (2019) 105952

Contents lists available at ScienceDirect

International Immunopharmacology

journal homepage: www.elsevier.com/locate/intimp

Protective effects of a neurokinin 1 receptor antagonist on airway epithelial mitochondria dysfunction in asthmatic mice via Nrf2/HO-1 activation

Zhijia Wang, Miao Li, Qianlan Zhou, Yunxiao Shang*

Department of Paediatrics, Shengjing Hospital of China Medical University, Shenyang 110004, People's Republic of China

1. Introduction

Bronchial asthma is a heterogeneous disease characterized by chronic airway inflammation with significant morbidity and mortality. Airway epithelial damage plays a crucial role in the pathogenesis of asthma [1–3]. The activation of airway epithelial cells can promote the Th2 immune response, secretion of a series of cytokines, and release of numerous inflammatory cells, such as eosinophils, lymphocytes, and macrophages. These inflammatory cells aggregate in the airways, wherein they are activated, causing further damage to the epithelium and release of a large amount of oxygen free radicals, causing oxidative stress [4–6]. Epithelial damage activates epithelial-mesenchymal repair, leading to airway remodeling [7,8], and mitochondria are the most important source of endogenous reactive oxygen species (ROS) [9]. The inhibition of mitochondrial damage, which in turn inhibits oxidative stress, is an effective method to reduce epithelial cell damage and inhibit airway remodeling and may be a new breakthrough strategy in asthma treatment [10–12].

SP is a sensory neuropeptide closely associated with asthma [13–17]. In the airway, SP mainly exerts biological activity by binding to its specific receptor, NK-1R, which is mainly found in the tracheal epithelium, around the bronchial smooth muscle, and surrounding the vascular smooth muscle and submucosal glands [18]. Studies have shown that SP is closely associated with oxidative stress [19] and can induce the release of mitochondrial-derived ROS in the airway epithelia of asthmatic mice [20].

Nuclear factor-erythroid 2-related factor 2 (Nrf2) is a transcription factor with antioxidant and anti-inflammatory properties that is involved in mitochondrial function regulation and plays an important role in improving asthma airway inflammation and oxidative stress [21]. Oxidative stress causes Nrf2 to dissociate from Kelch-like epoxy chloropropane-associated protein-1 (Keap1), and the Nrf2 nuclear localization signal induces its rapid translocation to the nucleus for activation. Upon entry into the nucleus, Nrf2 binds to the antioxidant response element (ARE) and initiates the transcription of multiple protective downstream genes [22,23]. Among these genes is heme oxygenase-1 (HO-1), an important endogenous antioxidant and cytoprotective enzyme [24–27]. During the onset of allergic asthma, the expression of HO-1 in the lung tissue is increased [28]. Activation of Nrf2/HO-1 has a protective effect against mitochondrial damage [29].

We herein aimed to investigate the effects and mechanisms of an NK-1R antagonist (WIN 62,577) against airway epithelial mitochondria damage in a mouse asthmatic model in vivo and in IL-13-induced 16HBE cells in vitro.

2. Materials and methods

2.1. Animals and groups

Female BALB/c mice (age, 6–7 weeks; weight, 18–20 g) were purchased from Liaoning Changsheng Biotechnology Co., Ltd. and raised in the Specific-pathogen free animal room of the Benxi Experimental Base of Shengjing Hospital affiliated with China Medical University. The treatment of experimental animals was approved by the Ethics Committee of Shengjing Hospital affiliated with China Medical University.

After acclimatization for one week, the animals were randomly divided into 4 groups: a control group, asthmatic group, WIN 62,577 group (NK-1R antagonist, Sigma-Aldrich, USA), and hexadecadrol group. Hexadecadrol was used as a positive control. Animals in the asthmatic, WIN 62,577 and hexadecadrol groups were intraperitoneally injected with 0.2 ml of an OVA sensitization solution (containing OVA (50 μg, Sigma-Aldrich) and aluminum hydroxide (2 mg, Shenyang Chemical Third Factory, China)) on days 0, 7, and 14; animals in the control group were intraperitoneally injected with 0.2 ml of phosphate-buffered saline (PBS). Next, animals in the asthmatic, WIN 62,577 and hexadecadrol groups were given an OVA challenge solution (4% OVA solution) by inhalation once a day for 30 min from 21 d to 28 d for 7 consecutive days, and those in the control group inhaled PBS. One hour before each challenge, animals in the WIN 62,577 group were intraperitoneally injected with WIN 62,577 300 μg, and those in the hexadecadrol group were intraperitoneally injected with hexadecadrol (2 mg/kg, Rongsheng Pharmaceutical Co., Ltd., China). The control and asthmatic group animals were given PBS.

* Corresponding author at: Department of Paediatrics, Shengjing Hospital of China Medical University, 36 Sanhao Street, Shenyang 110004, People's Republic of China.

E-mail address: shangyunxiao827@163.com (Y. Shang).

https://doi.org/10.1016/j.intimp.2019.105952
Received 4 August 2019; Received in revised form 11 September 2019; Accepted 30 September 2019
Available online 31 October 2019

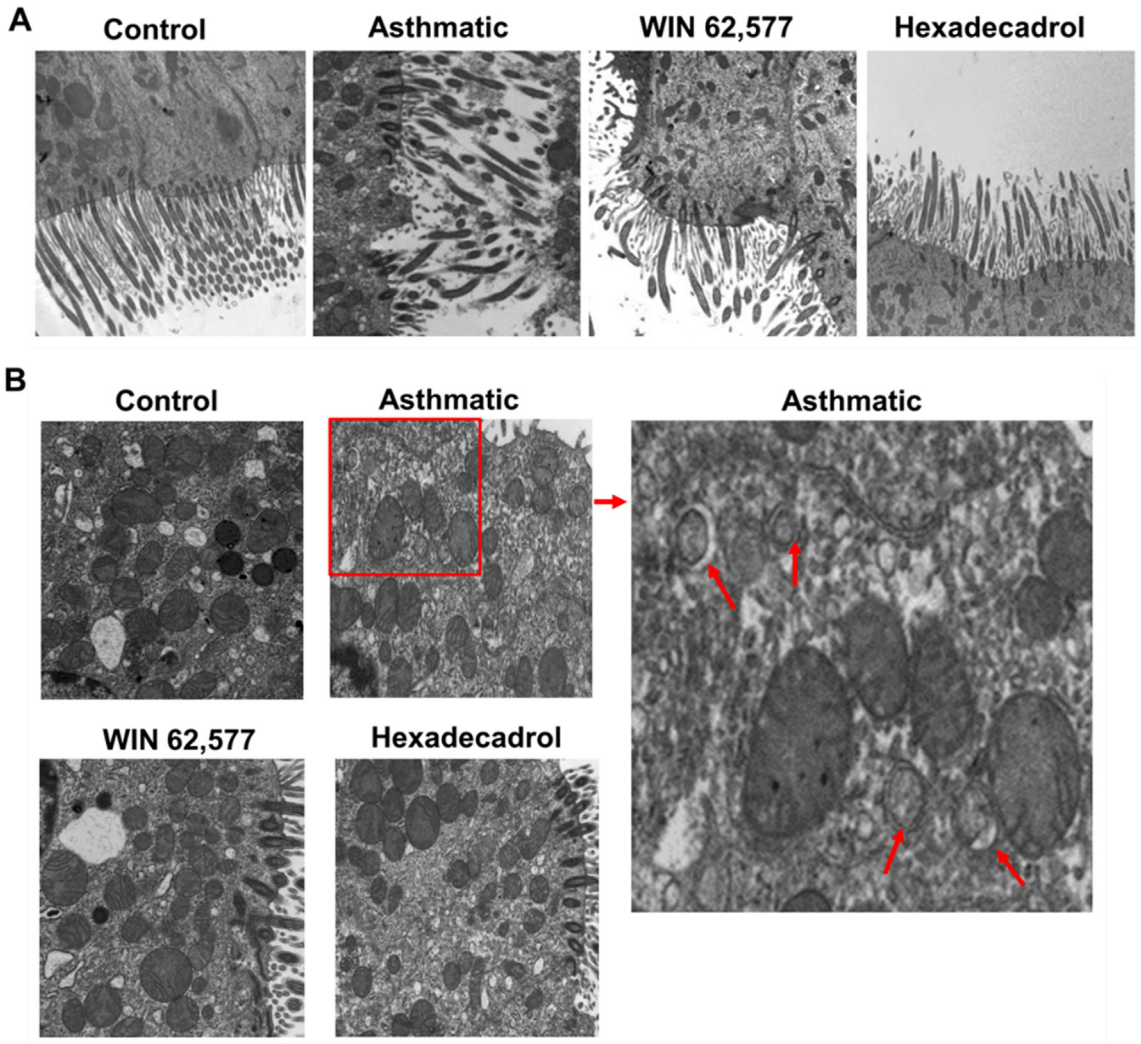

Fig. 1. Ultrastructural changes in the mouse airway epithelium. (A) Changes in the cilia of the airway epithelium. In the asthmatic group, the epithelial cilia were ruptured, detached, disordered and irregular. In the WIN 62,577 and hexadecadrol groups, tracheal epithelial cilia damage was alleviated. (B) Mitochondrial changes in the airway epithelium. The number of mitochondria in the epithelial cells of the asthmatic group was increased, the density was decreased, mitochondrial cristae were disrupted or absent, and autophagic bodies were observed (indicated by red arrows). Mitochondrial structural damage was reduced in the WIN 62,577 and hexadecadrol groups.

2.2. Transmission electron microscopy

The ultrastructural changes in the ciliary epithelia and mitochondria in mice were observed by transmission electron microscopy. The mouse trachea was removed and fixed in 2.5% glutaraldehyde for 2 h and 1% citric acid for 2 h and then dehydrated in graded dilutions of ethanol and acetone. The tissue was embedded, and ultrathin sections (50 nm) were cut. Dual staining of acetic acid-lead citrate was performed, and sections were observed and photographed with a transmission electron microscope (H-7650, HITACHI, Japan).

2.3. Mitochondrial isolation

Immediately after sacrifice, fresh lung tissues were stored on ice, and a tissue mitochondrial isolation kit (Beyotime Biotechnology, China) was used. First, tissue samples were suspended in precooled mitochondrial separation reagent A (10 volumes), homogenized and centrifuged at 600*g* at 4 °C for 5 min. The supernatant was retained and centrifuged at 11,000*g* at 4 °C for 10 min. Next, the supernatant was discarded, and the precipitate was retained as the isolated mitochondria.

2.4. Mitochondrial membrane potential detection (JC-1)

A mitochondrial membrane potential detection kit (JC-1, Beyotime Biotechnology, China) was used. First, a JC-1 staining working solution was prepared, and 0.9 ml of a 5-fold-diluted JC-1 staining working solution was added to 0.1 ml of purified mitochondria with a total protein amount of 50 μg. The solution was mixed well, and the fluorescence was recorded by a fluorescence microplate reader. In addition, the cells were observed under a fluorescence microscope, and pictures were taken at 200× magnification.

2.5. ROS determination (DCFH-DA assay)

Using an ROS assay kit (Nanjing Institute of Bioengineering, China), mouse lung tissue was first prepared as a single-cell suspension, whereas 16HBE cells were directly assayed in vitro. First, the lung tissue was treated with trypsin and digested at 37 °C for 30 min. Then, the tissue pieces were removed by filtration through a 300 nylon mesh, and the filtered cells were collected and centrifuged at 500*g* for 10 min. The supernatant was removed, and the single-cell suspension was resuspended. DCFH-DA (10 μM) was added to the single-cell suspension. After incubation at 37 °C for 1 h, the cells were centrifuged at 1000*g* for

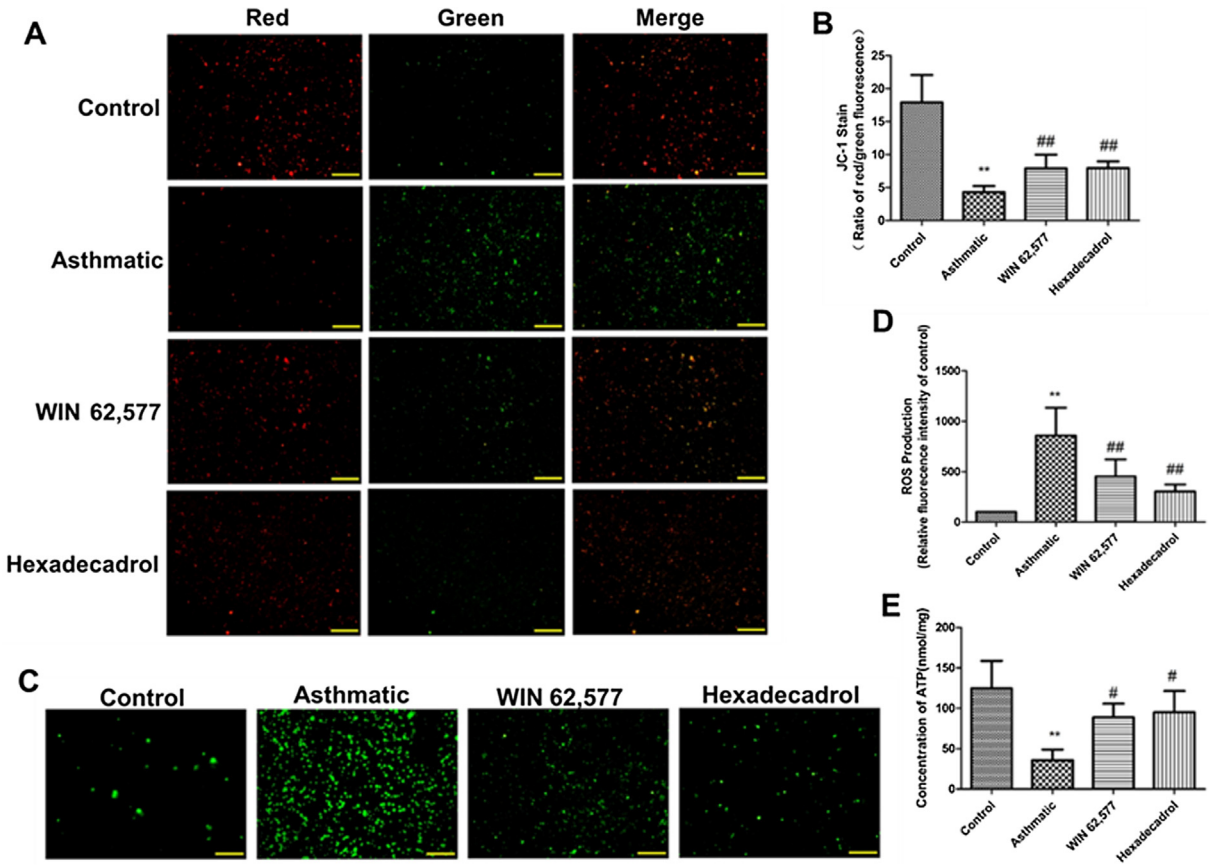

Fig. 2. Protective effect of WIN 62,577 against airway mitochondrial dysfunction in asthmatic mice. (A) WIN 62,577 treatment inhibits the decrease in mitochondrial membrane potential in asthmatic mice (JC-1, ×200). (B) Relative proportion of red/green fluorescence. (C) WIN 62,577 treatment inhibits ROS production in asthmatic mice (DCFH-DA, × 200). (D) Relative fluorescence intensity of ROS. (E) WIN 62,577 treatment inhibits the ATP decrease in asthmatic mice; the ATP concentration is expressed as nmol/mg. Each value represents the mean ± SD (n = 8). $^{**}P < 0.01$ versus the control group. $^{\#}P < 0.05$, $^{\#\#}P < 0.01$ versus the asthmatic group.

10 min and washed 3 times with serum-free cell culture medium. The fluorescence was detected by a microplate reader, and fluorescence microscopy images were captured at 200× magnification.

2.6. Adenosine triphosphate (ATP) detection

ATP was measured with an Enhanced ATP Assay kit (Beyotime Biotechnology, China). The lung tissue was added to the lysis buffer and centrifuged at 12,000*g* for 5 min at 4 °C, and the supernatant was retained. After preparation of the ATP test solution, 100 μl was added to each well of a 96-well plate according to the order of detection. After 5 min of incubation at room temperature, 20 μl of the sample or standard was added to the test well, mixed quickly, and read using a multifunctional microplate reader after 2 s. The relative light unit (RLU) value was determined.

2.7. Western blot analysis

Cytoplasmic, nuclear, and total proteins were extracted, and the protein concentrations were assessed with a BCA assay. Equal quantities of protein samples were then resolved on 10% acrylamide sodium dodecyl sulfate-polyacrylamide gel electrophoresis (SDS-PAGE) gels and transferred to polyvinylidene fluoride (PVDF) membranes. The membranes were blocked with 5% skim milk for 2 h and incubated with the diluted antibody with agitation overnight at 4 °C. The antibody dilution ratios were as follows: Nrf2 antibody (Cell Signaling Technology, USA), 1:1000; HO-1 antibody (Cell Signaling Technology, USA), 1:1000; β-actin antibody (Proteintech, Wuhan, China), 1:1000; and histone H3 antibody (Proteintech, Wuhan, China), 1:1000. Then, the membranes were incubated with a 1:5000 dilution of goat anti-rabbit IgG-HRP secondary antibody for 2 h, washed 3 times with TBST, incubated with ECL chemiluminescence liquid (Thermo Pierce, USA) and exposed in a dark room.

2.8. Cell culture and groups

Human bronchial epithelial 16HBE cells (Xiangya Medical College Cell Bank, China) were cultured in RPMI 1640 medium (HyClone, USA) supplemented with 10% fetal bovine serum and 1% penicillin/streptomycin at 37 °C and 5% CO_2. The cells were cultured until they reached 70% confluence. Control group cells were cultured normally, and those in the IL-13, IL-13 + SP, and IL-13 + WIN 62,577 groups were treated with recombinant human IL-13 (25 ng/ml, Peprotech, USA) for 48 h. After 48 h, cells in the IL-13 + SP group were treated with substance P (10 nM, Abcam, USA) for 1 h, and those in the IL-13 + WIN 62,577 group were treated with WIN 62,577 (10 nM) for 1 h.

2.9. Immunofluorescence staining

Each group of cells was grown on cover glass and fixed with 4% paraformaldehyde for 15 min. The 4% paraformaldehyde was removed, and the fixed cells were washed 3 times with PBS. The cells were completely covered with 0.1% Triton X-100 and incubated for 30 min at room temperature. The 0.1% Triton X-100 was removed, and the cells were washed 3 times with PBS. Goat serum was added and incubated for 15 min at room temperature, after which a diluted Nrf2 antibody

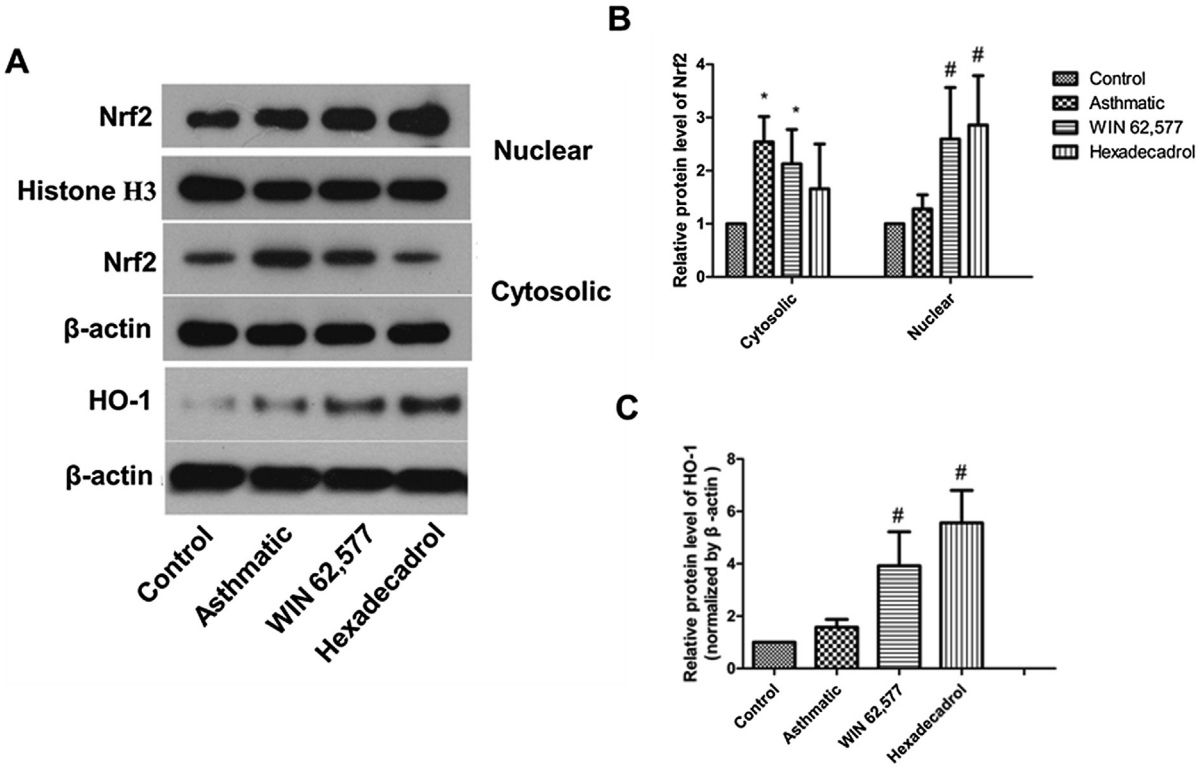

Fig. 3. Effect of WIN 62,577 on the expression of Nrf2/HO-1 in the lung tissues of asthmatic mice. (A) Nrf2 and HO-1 protein expression was detected by Western blot. (B) and (C) Densitometric analyses of Nrf2 and HO-1 normalized to histone H3 or β-actin. Each value represents the mean ± SD (n = 3). $^{*}P < 0.05$ versus the control group. $^{\#}P < 0.05$ versus the asthmatic group.

(1:200) was added and incubated at 4 °C overnight. Next, a diluted Cy3-labeled goat anti-rabbit IgG (1:200) secondary antibody was added and incubated for 1 h at room temperature in the dark. Subsequently, the stained cells were washed 3 times with PBS, and nuclei were stained with DAPI for 5 min. The stained cells were photographed under a fluorescence microscope at 400× magnification.

2.10. Nrf2 shRNA transfection

The Nrf2 shRNA plasmid (Shanghai Genechem Co., Ltd., China) was constructed, and cells were seeded in a 6-well plate according to the experimental group; transfection was performed 24 h later. The transfection medium was discarded, serum-free medium was added, and the cells were incubated for 1 h at 37 °C in a 5% CO_2 incubator. Opti-MEM solution (100 μl) with liposome 2000 (8 μl) and Opti-MEM solution (100 μl) with an Nrf2 shRNA plasmid or negative control plasmid (2 μg) were incubated for 5 min at room temperature. Then, two groups of solutions were mixed thoroughly and incubated at room temperature for 20 min. The mixture was added dropwise to the wells, and the cells were cultured at 37 °C in a 5% CO_2 incubator for 4 h.

2.11. Reverse transcription and quantitative real-time polymerase chain reaction (RT-qPCR)

After transfection, the expression of Nrf2 mRNA was detected by RT-qPCR. First, total RNA was extracted with TRIzol (Takara Bio Inc., China), and reverse transcription was carried out using a PrimeScript RT reagent kit (Takara Bio Inc., China). qPCR was performed using a SYBR Premix Ex kit (Takara Bio Inc., China) and an ABI PRISM7500 Real-Time system (Life, USA). The primer sequences were as follows: Nrf2 (forward-5′- GTCAGCGACGGAAAGAGTA-3′ and reverse-5′- ACC TGGGAGTAGTTGGCA-3′) and β-actin (forward-5′- CTTAGTTGCGTTA CACCCTTTCTTG-3′ and reverse-5′-CTGTCACCTTCACCGTTCCAG TTT-3′). β-Actin was used as an internal reference gene to normalize the expression of Nrf2. Expression levels were calculated using the $2^{-\Delta\Delta}$CT method.

2.12. Statistical analysis

Statistical analysis was performed using SPSS 21.0 software. The results were repeated at least three times. Measurement data are presented as the mean ± standard deviation ($\bar{x} \pm s$). Comparisons between groups were analyzed by one-way analysis of variance (ANOVA). $P < 0.05$ was considered significant.

3. Results

3.1. Ultrastructural changes in the mouse airway epithelium

The airway epithelial ultrastructure in each group was observed by transmission electron microscopy. The cilia of the tracheal epithelium were in an orderly and regular arrangement without detachment in the control group. In contrast, in the asthmatic group, the epithelial cilia were ruptured, detached, disordered, and irregular, and goblet cell infiltration was increased; compared with that in the asthmatic group, the WIN 62,577 and hexadecadrol groups showed reduced tracheal-ciliated epithelial damage (Fig. 1A).

In addition, we observed ultrastructural changes in the mitochondria of the tracheal epithelium. In the control group, the density of the mitochondrial matrix was uniform, and the mitochondrial ridge was clear. Compared with the control group, in the asthmatic group, the number of mitochondria in the epithelial cells was increased, the mitochondria were swollen, the density was decreased, mitochondrial vacuolation was present, mitochondrial cristae were disrupted or absent, and autophagic bodies were observed. However, mitochondrial structural damage was reduced in the WIN 62,577 and hexadecadrol groups (Fig. 1B).

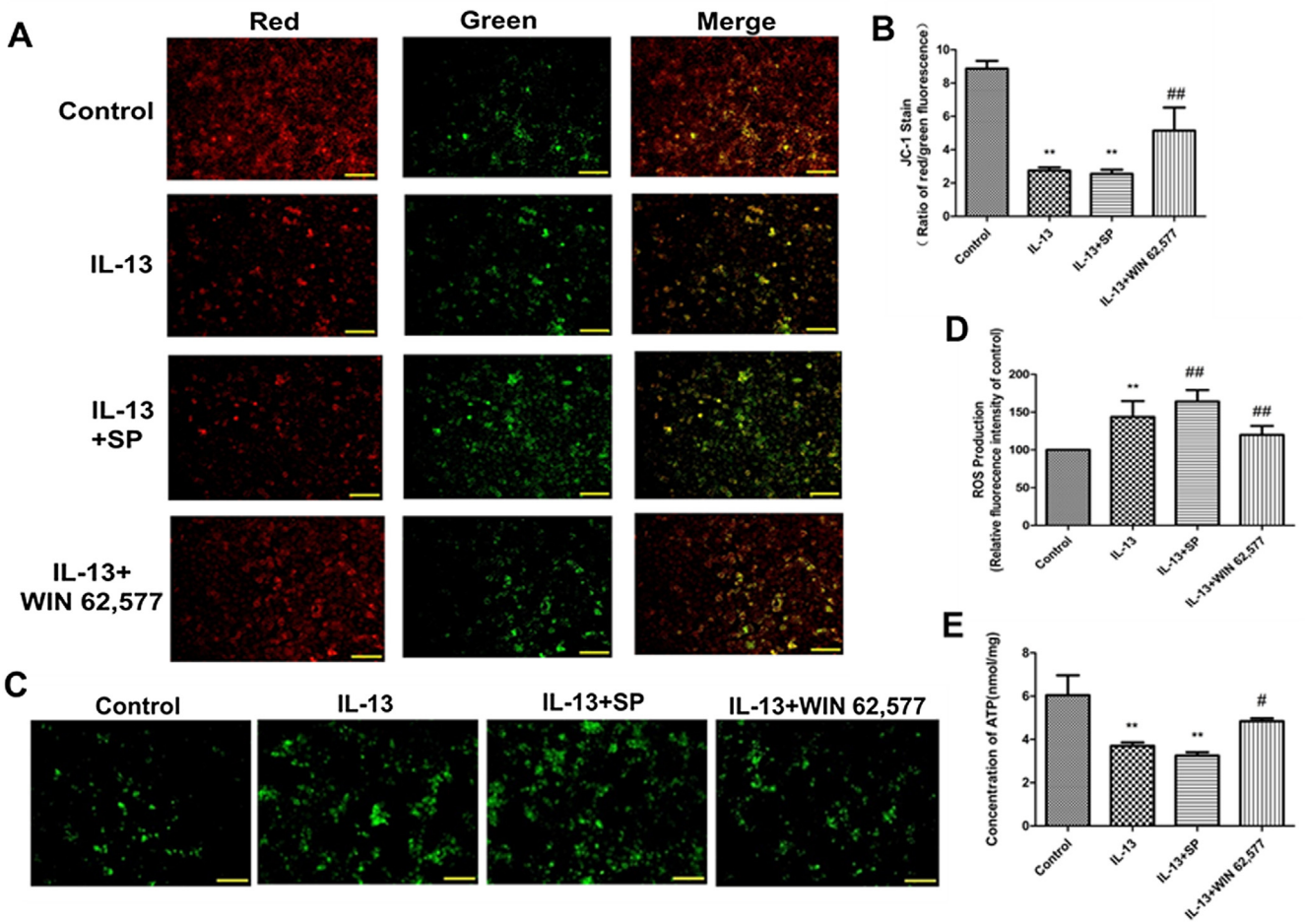

Fig. 4. Protective effect of WIN 62,577 against mitochondrial dysfunction in IL-13-induced 16HBE cells. (A) JC-1 fluorescence staining (×200). Compared with that in the IL-13 group, the proportion of red fluorescence was increased significantly in the IL-13 + WIN 62,577 group. (B) The red/green fluorescence intensity ratios. (C) Effect of WIN 62,577 treatment on the ROS levels in IL-13-induced 16HBE cells, as assessed by DCFH-DA fluorescence detection (×200). The green fluorescence signal was increased in the IL-13 and IL-13 + SP groups and decreased significantly after WIN 62,577 treatment. (D) Relative ROS fluorescence intensity. (E) WIN 62,577 treatment inhibited the ATP reduction in IL-13-induced 16HBE cells; the ATP concentration is expressed as nmol/mg. Each value represents the mean ± SD (n = 3). $^{**}P < 0.01$ versus the control group. $^{\#}P < 0.05$, $^{\#\#}P < 0.01$ versus the asthmatic group.

3.2. Protective effect of the NK-1R antagonist WIN 62,577 against airway mitochondrial dysfunction in asthmatic mice

3.2.1. WIN 62,577 inhibited the mitochondrial membrane potential decrease in asthmatic mice

To investigate the changes in mitochondrial function, we first detected the mitochondrial membrane potential levels in each group. High mitochondrial membrane potential results in the aggregation of JC-1 in the mitochondrial matrix and polymer formation (J-aggregates), which can produce red fluorescence. Low mitochondrial membrane prohibits JC-1 aggregation in the mitochondrial matrix, and JC-1 remains as a monomer, which can produce green fluorescence. Thus, the change in mitochondrial membrane potential can be detected by a shift in fluorescence. In the control group, JC-1 aggregated in the normal mitochondria and showed red fluorescence. In the asthmatic group, the relative proportion of red/green fluorescence decreased significantly compared with that of the control group ($P < 0.01$), indicating that the mitochondrial membrane potential had decreased. Compared with the asthmatic group, the relative proportion of red/green fluorescence in WIN 62,577 group increased significantly ($P < 0.01$), indicating that WIN 62,577 treatment inhibited the decrease in mitochondrial membrane potential in the lung tissues of asthmatic mice (Fig. 2A&B).

3.2.2. WIN 62,577 inhibited ROS production in asthmatic mice

In addition, we measured the ROS levels in each group to reflect mitochondrial damage. ROS can oxidize nonfluorescent DCFH to produce green fluorescent DCF. As shown in Fig. 2C&D, the green fluorescence of the asthmatic group was increased significantly ($P < 0.01$), indicating an increase in ROS production. In contrast, compared with that in the asthmatic group, the green fluorescence in the WIN 62,577 group was decreased significantly ($P < 0.01$), indicating that ROS production was decreased. These results suggest that WIN 62,577 treatment inhibits ROS production in the lung tissues of asthmatic mice and may alleviate mitochondrial damage.

3.2.3. WIN 62,577 inhibited ATP reduction in asthmatic mice

We further examined the ATP levels in each group because mitochondria play a central role in energy metabolism and, importantly, synthesize ATP during oxidative phosphorylation. Therefore, a decrease in ATP levels indicates that mitochondrial function is impaired or reduced. The concentration of ATP in the lung tissues of asthmatic group mice was significantly lower than that in the lung tissues of control group mice ($P < 0.01$), indicating that the mitochondrial function was impaired in the lung tissues of asthmatic mice. Conversely, compared with that in the asthmatic group, the ATP concentration in the WIN 62,577 intervention group was increased ($P < 0.05$) (Fig. 2E), indicating that WIN 62,577 could inhibit the decrease in ATP in asthmatic

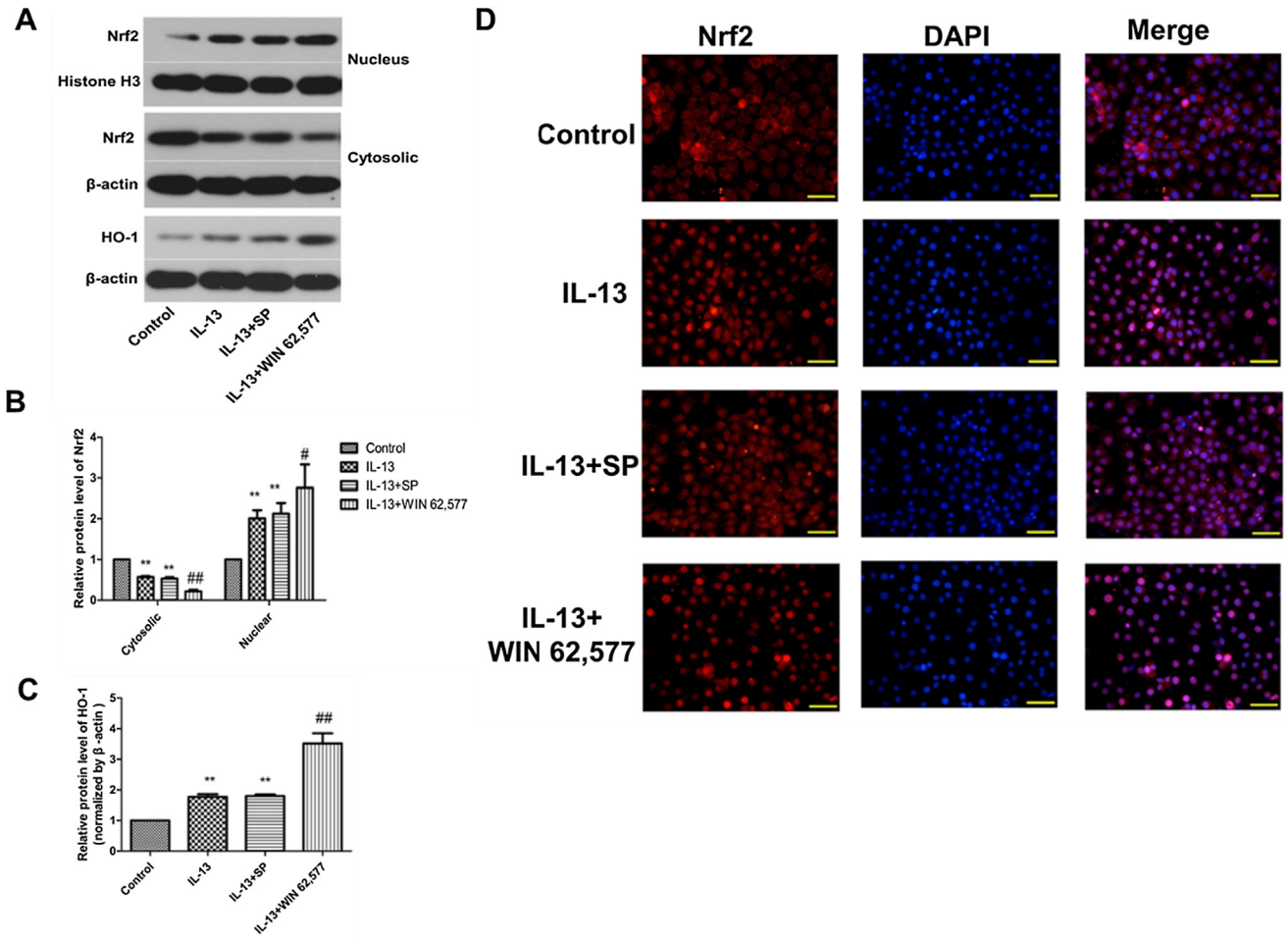

Fig. 5. WIN 62,577 activates Nrf2/HO-1 in IL-13-induced 16HBE cells. (A) Western blot showing the effects of WIN 62,577 on the expression of Nrf2 and HO-1 in IL-13-induced 16HBE cells. (B & C) Densitometric analyses of Nrf2 and HO-1 normalized to histone H3 or β-actin. (D) The translocation of Nrf2 in 16HBE cells was determined by immunofluorescence staining (×400). Nrf2 is shown by red fluorescence, and DAPI is shown in blue. In the control group, Nrf2 was mainly expressed in the cytoplasm. WIN 62,577 treatment increased the nuclear translocation and activation of Nrf2 in IL-13-induced 16HBE cells. Each value represents the mean ± SD (n = 3). $^{**}P < 0.01$ versus the control group. $^{\#}P < 0.05$, $^{\#\#}P < 0.01$ versus the asthmatic group.

mice. These results suggest that WIN 62,577 can alleviate mitochondrial dysfunction in asthmatic mice.

3.3. The NK-1R antagonist WIN 62,577 activated Nrf2/HO-1 in the lung tissues of asthmatic mice

To further explore the possible mechanism of WIN 62,577 in alleviating airway mitochondrial dysfunction in asthmatic mice, we detected the expression of Nrf2 and its downstream protein HO-1 by Western blot. As shown in Fig. 3, in the WIN 62,577 intervention group, the expression of Nrf2 protein in the nucleus was increased compared with the asthmatic group ($P < 0.05$), indicating that WIN 62,577 activated Nrf2 in mouse lung tissue. Nrf2 activation further activates the transcription of many downstream protective genes, among which HO-1 is an important endogenous antioxidant and cytoprotective enzyme that is closely associated with asthma [28]. Similarly, we found that the expression of HO-1 protein in the lung tissue of the mice in the WIN 62,577 intervention group was up-regulated compared to that in the asthmatic group ($P < 0.05$).

3.4. Protective effect of the NK-1R antagonist WIN 62,577 against mitochondrial dysfunction in IL-13-induced 16HBE cells

In addition, human bronchial epithelial cell line 16HBE was used for in vitro experiments. IL-13, one of the most important cytokines in the pathogenesis of asthma, is mainly secreted by activated Th2 cells and has many biological effects. IL-13 can induce all of the symptoms of asthma, which are closely related to airway inflammation, airway hyperresponsiveness and airway remodeling, without input from other cytokines [30,31]. Therefore, we induced 16HBE cells with IL-13 for in vitro experiments.

3.4.1. WIN 62,577 inhibited the mitochondrial membrane potential decrease in IL-13-induced 16HBE cells

First, in vitro experiments were conducted to observe the effect of WIN 62,577 on IL-13-induced mitochondrial membrane potential. Compared with the control group, the ratio of red/green fluorescence in the IL-13 group was significantly decreased ($P < 0.01$), indicating that IL-13 induction could cause a decrease in mitochondrial membrane potential. On the contrary, the red/green fluorescence ratio of WIN 62,577 intervention group was higher than that of the IL-13 induction group ($P < 0.05$), indicating that WIN 62,577 treatment could inhibit the decrease of mitochondrial membrane potential (Fig. 4A&B).

3.4.2. WIN 62,577 inhibited ROS production in IL-13-induced 16HBE cells

We then detected the effect of WIN 62,577 on the ROS levels in IL-13-induced 16HBE cells. As shown in Fig. 4C&D, the green fluorescence of the IL-13 group was increased significantly compared with that of the control group ($P < 0.01$), indicating that IL-13 treatments stimulated the release of ROS from 16HBE cells. We also found that SP could

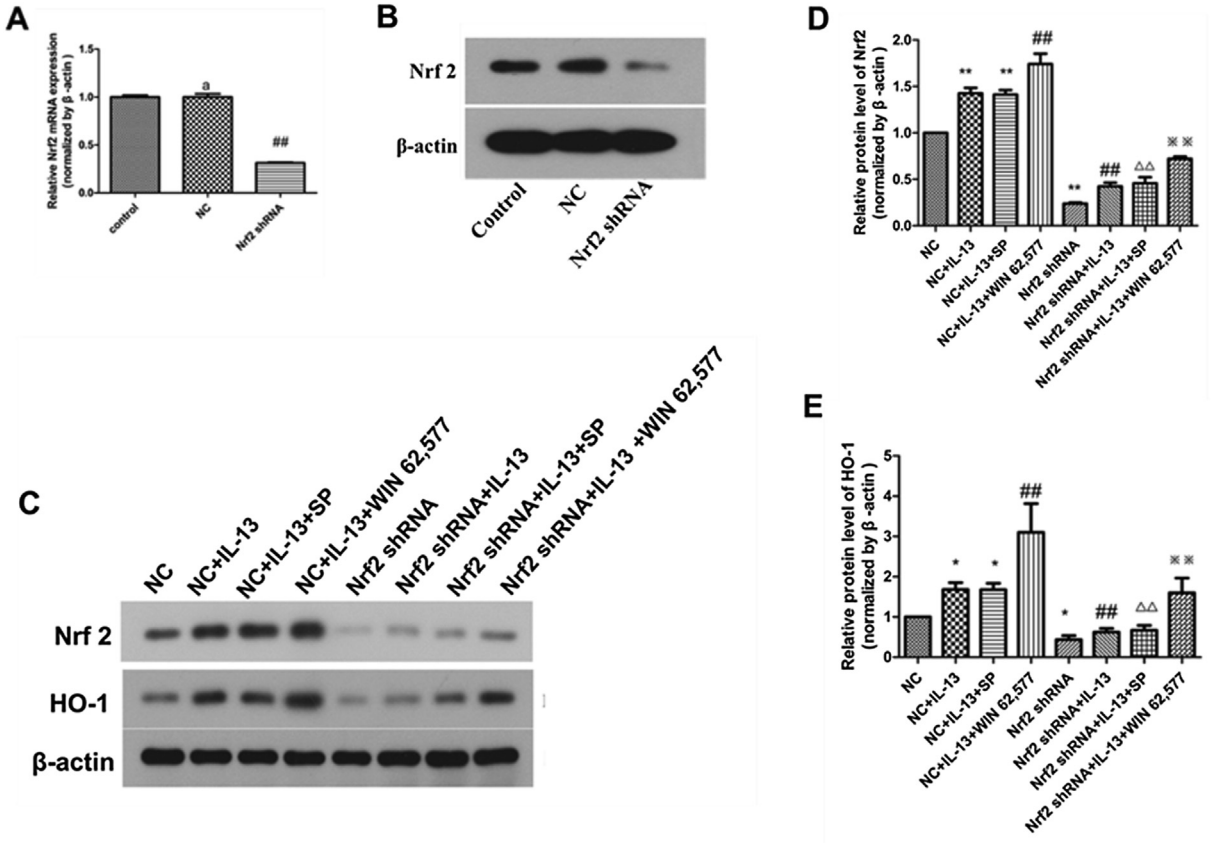

Fig. 6. The effect of Nrf2 shRNA transfection on the protein expression of Nrf2 and HO-1. (A) The differences in Nrf2 gene expression were detected by RT-PCR. NC or Nrf2 shRNA was transfected into 16HBE cells. The mRNA expression levels in all PCR samples were normalized to β-actin mRNA. (B) Western blotting was used to verify the transfection effect. (C) The protein expression levels of Nrf2 and HO-1 in each group after transfection were detected by Western blot. (D, E) Densitometric analyses of Nrf2 and HO-1. Each value represents the mean ± SD (n = 3). $^{a}P > 0.05$ versus the control group. $^{*}P < 0.05$, $^{**}P < 0.01$ versus the NC group. $^{\#\#}P < 0.01$ versus the NC + IL-13 group. $^{\Delta\Delta}P < 0.01$ versus the NC + IL-13 + SP group. $^{\divideontimes\divideontimes}P < 0.01$ versus the NC + IL-13 + WIN 62,577 group.

further increase the ROS released from IL to 13-induced 16HBE cells ($P < 0.01$), while the green fluorescence was significantly decreased after intervention with WIN 62,577 ($P < 0.01$), suggesting that WIN 62,577 could inhibit the release of ROS from IL to 13-induced 16HBE cells.

3.4.3. WIN 62,577 inhibited the ATP reduction in IL-13-induced 16HBE cells

We further measured the ATP levels and found that compared with the control group, the IL-13-induced 16HBE group showed a significantly decreased ATP concentration ($P < 0.01$). The concentration of ATP in the WIN 62,577 intervention group was higher than that in the IL-13 induction group ($P < 0.05$) (Fig. 4E). The results showed that WIN 62,577 could inhibit the decrease of ATP induced by IL-13.

3.5. The NK-1R antagonist WIN 62,577 activated Nrf2/HO-1 in IL-13-induced 16HBE cells

To further verify the protective mechanism of WIN 62,577 on mitochondria, we detected the expression of Nrf2 and HO-1 by Western blot (Fig. 5A-C). The expression of Nrf2 in the nucleus and HO-1 expression was increased after WIN 62,577 treatment compared with that in the IL-13 induction group, suggesting that WIN 62,577 activates Nrf2 and up-regulates HO-1 expression in IL-13-induced 16HBE cells. The immunofluorescence results further showed that WIN 62,577 could promote Nrf2 migration from the cytoplasm to the nucleus in 16HBE cells induced by IL-13, indicating that Nrf2 was further activated (Fig. 5D).

3.6. Effect of Nrf2 shRNA transfection on the protein expression of Nrf2 and HO-1

Nrf2 shRNA and negative control (NC) plasmids were transfected into 16HBE cells, and the cells were divided into three groups: a control group, NC group and Nrf2 shRNA group. The Nrf2 mRNA expression in each group was detected by RT-PCR after 24 h. No significant difference in Nrf2 mRNA expression was observed between the NC group and the control group ($P > 0.05$). Compared with that in the NC group, the Nrf2 mRNA expression in the Nrf2 shRNA group was significantly decreased ($P < 0.01$) (Fig. 6A). Similarly, Western blotting was performed 48 h after transfection, revealing no significant difference in the protein expression of Nrf2 between the NC group and the control group ($P > 0.05$); the protein expression of Nrf2 in the Nrf2 shRNA group was significantly lower than that in the NC group ($P < 0.01$) (Fig. 6B). These results suggest that the transfection was successful.

Then, the NC or Nrf2 shRNA plasmid was transfected, and the cells were treated accordingly. The cells were divided into 8 groups: an NC group, NC + IL-13 group, NC + IL-13 + SP group, NC + IL-13 + WIN 62,577 group, Nrf2 shRNA group, Nrf2 shRNA + IL-13 group, Nrf2 shRNA + IL-13 + SP group, and Nrf2 shRNA + IL-13 + WIN 62.577 group. The protein expression of Nrf2 and HO-1 in each group after transfection was detected by Western blot. The protein expression of Nrf2 and HO-1 in cells transfected with Nrf2 shRNA was lower than that in the NC group (Fig. 6C-E).

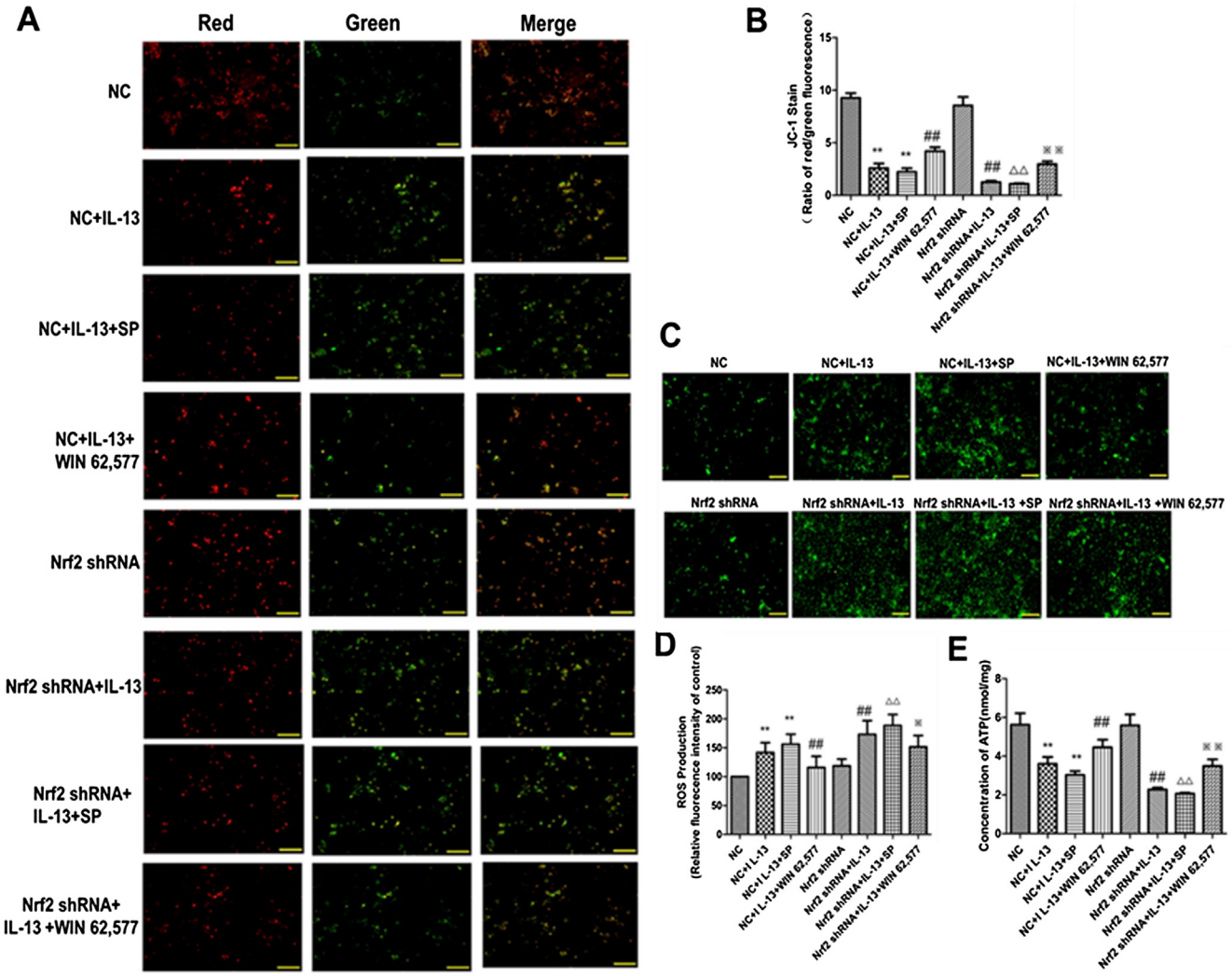

Fig. 7. Transfection of Nrf2 shRNA inhibits the WIN 62,577-mediated protection of mitochondria in IL-13-induced 16HBE cells. (A) Effect of Nrf2 shRNA transfection on mitochondrial membrane potential (JC-1, ×200). The green fluorescence intensity was increased, and the red fluorescence intensity was decreased in each group after transfection of Nrf2 shRNA, indicating that the mitochondrial membrane potential was decreased. (B) The ratio of red-to-green fluorescence intensity. (C) The effect of Nrf2 shRNA transfection on the ROS levels in each group (DCFH-DA, ×200). The green fluorescence intensity in each group was increased after transfection of Nrf2 shRNA, indicating that the ROS production was increased. (D) Relative fluorescence intensity of ROS. (E) After transfection of Nrf2 shRNA, the ATP concentration in each group was decreased. Each value represents the mean ± SD (n = 3). $^{**}P < 0.01$ versus the NC group. $^{\#\#}P < 0.01$ versus the NC + IL-13 group. $^{\Delta\Delta}P < 0.01$ versus the NC + IL-13 + SP group. $^{\divideontimes}P < 0.05$, $^{\divideontimes\divideontimes}P < 0.01$ versus the NC + IL-13 + WIN 62,577 group.

3.7. Transfection of Nrf2 shRNA inhibits the WIN 62,577-mediated protection of mitochondria in IL-13-induced 16HBE cells

3.7.1. Transfection of Nrf2 shRNA inhibits WIN 62,577-mediated protection against mitochondrial membrane potential decrease in IL-13-induced 16HBE cells

After transfection of the NC or Nrf2 shRNA plasmid, the mitochondrial membrane potential was detected by JC-1 fluorescence. Compared with that in the corresponding NC group, the green fluorescence intensity was increased, and the red fluorescence intensity was decreased in each group after transfection of Nrf2 shRNA, indicating that the mitochondrial membrane potential was decreased in each group after transfection of Nrf2 shRNA (Fig. 7A & B). These findings suggest that inhibition of Nrf2 expression inhibits the WIN 62,577-mediated protection of the mitochondrial membrane potential in IL-13-induced 16HBE cells.

3.7.2. The WIN 62,577-mediated inhibition of ROS production in IL-13-induced 16HBE cells is inhibited by Nrf2 shRNA transfection

We further tested the levels of ROS (DCFH-DA) in each group after transfection. The green fluorescence intensity was increased in each group transfected with Nrf2 shRNA compared with those in the corresponding group transfected with NC plasmid, indicating an increase in ROS production in each group transfected with Nrf2 shRNA (Fig. 7C & D). These results suggest that the inhibition of Nrf2 expression by Nrf2 shRNA transfection reduces the WIN 62,577-mediated inhibition of ROS production in IL-13-induced 16HBE cells.

3.7.3. Transfection of Nrf2 shRNA inhibits the inhibition of ATP reduction in IL-13-induced 16HBE cells by WIN 62,577

Similarly, we tested changes in ATP levels after transfection in each group, revealing that the ATP levels were significantly lower in each group transfected with Nrf2 shRNA compared with those in the corresponding groups transfected with NC plasmid (Fig. 7E). These results suggest that transfection of Nrf2 shRNA rescues the WIN 62,577-mediated ATP reduction in IL-13-induced 16HBE cells.

4. Discussion

Asthma is a common chronic respiratory disease, and its incidence

and prevalence are still increasing globally, especially in developing countries. Therefore, in-depth research and exploration of new and effective treatments are urgently required.

In this study, we found that an NK-1R antagonist could up-regulate the expression of Nrf2/HO-1 in vivo and in vitro, representing a potential mechanism for the protective effect of an NK-1R antagonist on mitochondrial dysfunction.

First, we found that the NK-1R antagonist WIN 62,577 could alleviate damage to the airway epithelial cilia and mitochondrial structure in asthmatic mice to some extent. In vitro, transmission electron microscopy showed that the epithelial cilia structure was destroyed in asthmatic mice, indicating that the epithelial barrier of asthmatic mice was perturbed. The mitochondrial structure in the epithelia of asthmatic mice was also changed markedly, as swelling, decreased density, disruption or absence of mitochondrial cristae, and autophagic bodies were observable. Structural changes are mainly due to the damage of mitochondrial calcium transport function caused by ROS, resulting in calcium overload, activation of mitochondrial membrane permeability, opening of the transition pore, and increased mitochondrial membrane permeability, which further results in matrix edema, mitochondrial swelling and decreased density. In addition, the increase in autophagosomes indicates that to protect cells from ROS damage, damaged mitochondria releasing ROS are continuously removed via mitophagy [32]. However, after treatment with WIN 62,577, the epithelial cilia and mitochondrial structural damages were alleviated in asthmatic mice, and autophagosomes were also decreased significantly.

Then, we evaluated the protective effect of the NK-1R antagonist WIN 62,577 on mitochondrial function from three aspects: mitochondrial membrane potential, ROS and ATP levels. Mitochondrial membrane potential is negative inside and positive outside under normal conditions, which is the premise of the maintenance of mitochondrial oxidative phosphorylation and ATP production. Therefore, we can detect changes in mitochondrial membrane potential as a reflection of changes in mitochondrial function. WIN 62,577 inhibited the decrease in mitochondrial membrane potential in asthmatic mice and IL-13-induced 16HBE cells, reflecting a reduction in mitochondrial dysfunction. Oxidative stress is an imbalance between the oxidative system and antioxidant system, resulting in excessive ROS release, which is an important pathogenic feature of asthma [33,34]. Mitochondria are both a source of ROS production and a target for ROS attacks. ROS can damage the mitochondrial membrane and matrix, leading to mitochondrial dysfunction [35–37]. This study showed that ROS were increased significantly in the lung tissues of asthmatic mice, which may have been due to destruction of the respiratory chain in the mitochondria, resulting in increased ROS production and extensive molecular damage [38]. We also found that WIN 62,577 treatment could inhibit the release of ROS in the lung tissues of asthmatic mice and IL-13-induced 16HBE cells, thereby inhibiting oxidative stress damage and protecting mitochondrial function to some extent. Finally, we measured the ATP levels in each group because mitochondria play a central role in energy metabolism and, importantly, synthesize ATP during oxidative phosphorylation; thus, the decline in ATP levels can indicate impaired or decreased mitochondrial function. Our study found that WIN 62,577 treatment inhibited the ATP reduction in lung tissues and IL-13-induced 16HBE cells in asthmatic mice, suggesting that mitochondrial dysfunction was reduced.

To further investigate the mechanism by which NK-1R antagonists protect against mitochondrial dysfunction, we focused on the Nrf2/HO-1 pathway. Nrf2 is a transcription factor closely related to asthma and mitochondria that has antioxidant and anti-inflammatory effects. In the cytoplasm, Nrf2 binds to the inhibitory protein Keap1 in an inactive state. Oxidative stress and other factors cause Nrf2 to dissociate from Keap1 and rapidly translocate to the nucleus via the nuclear localization signal, wherein it is activated. We found that WIN 62,577 upregulated the expression of Nrf2/HO-1 in the lung tissues of asthmatic mice and IL-13-induced 16HBE cells. We also confirmed by immunofluorescence that WIN 62,577 promoted Nrf2 nuclear migration, indicating that Nrf2 is activated. In addition, we silenced the expression of the Nrf2 gene by transfecting 16HBE cells with Nrf2 shRNA in vitro and found that the protective effect of the NK-1R antagonist on mitochondrial dysfunction was reduced after transfection. This result indicates that the protective effect of the NK-1R antagonist on mitochondrial dysfunction was achieved by up-regulating Nrf2/HO-1. However, there are also some limitations to this study. The expression of other genes downstream of Nrf2 and whether NK-1R directly interacts with Nrf2 are still unclear, and further research is needed in the future.

In conclusion, this study found that an NK-1R antagonist exerts protective effects on mitochondrial dysfunction in the airway epithelia of asthmatic mice by up-regulating Nrf2/HO-1 expression, which may become a new breakthrough in the treatment of asthma.

Author contributions

Zhijia Wang, Miao Li and Yunxiao Shang designed this study, Zhijia Wang and Qianlan Zhou performed the experiments, Zhijia Wang performed the data analysis and interpretation, and Yunxiao Shang revised the manuscript. All authors read and approved the final paper.

Declaration of Competing Interest

The authors have no conflicts of interest to declare.

Appendix A. Supplementary material

Supplementary data to this article can be found online at https://doi.org/10.1016/j.intimp.2019.105952.

References

[1] S.N. Georas, F. Rezaee, Epithelial barrier function: at the front line of asthma immunology and allergic airway inflammation, J. Allergy Clin. Immunol. 134 (3) (2014) 509–520.
[2] S.T. Holgate, The sentinel role of the airway epithelium in asthma pathogenesis, Immunol. Rev. 242 (1) (2011) 205–219.
[3] B.N. Lambrecht, H. Hammad, Allergens and the airway epithelium response: gateway to allergic sensitization, J. Allergy Clin. Immunol. 134 (3) (2014) 499–507.
[4] J.L. Cho, M.F. Ling, D.C. Adams, et al., Allergic asthma is distinguished by sensitivity of allergen-specific CD4+ T cells and airway structural cells to type 2 inflammation, Sci. Transl. Med. 8 (359) (2016) 359ra132.
[5] C.D. Richards, Innate immune cytokines, fibroblast phenotypes, and regulation of extracellular matrix in lung, J. Interferon Cytokine Res. 37 (2) (2017) 52–61.
[6] D. Robinson, M. Humbert, R. Buhl, et al., Revisiting Type 2-high and Type 2-low airway inflammation in asthma: current knowledge and therapeutic implications, Clin. Exp. Allergy 47 (2) (2017) 161–175.
[7] O.A. Jaffer, A.B. Carter, P.N. Sanders, et al., Mitochondrial-targeted antioxidant therapy decreases transforming growth factor-beta-mediated collagen production in a murine asthma model, Am. J. Respir. Cell Mol. Biol. 52 (1) (2015) 106–115.
[8] S.J. Park, K.S. Lee, S.J. Lee, et al., L-2-Oxothiazolidine-4-carboxylic acid or alpha-lipoic acid attenuates airway remodeling: involvement of nuclear factor-kappaB (NF-kappaB), nuclear factor erythroid 2p45-related factor-2 (Nrf2), and hypoxia-inducible factor (HIF), Int. J. Mol. Sci. 13 (7) (2012) 7915–7937.
[9] V. Adam-Vizi, A.A. Starkov, Calcium and mitochondrial reactive oxygen species generation: how to read the facts, J. Alzheimers. Dis. 20 (Suppl 2) (2010) S413–426.
[10] U. Mabalirajan, A.K. Dinda, S. Kumar, et al., Mitochondrial structural changes and dysfunction are associated with experimental allergic asthma, J. Immunol. 181 (5) (2008) 3540–3548.
[11] U. Mabalirajan, A.K. Dinda, S.K. Sharma, et al., Esculetin restores mitochondrial dysfunction and reduces allergic asthma features in experimental murine model, J. Immunol. 183 (3) (2009) 2059–2067.
[12] P.H. Reddy, Mitochondrial dysfunction and oxidative stress in asthma: implications for mitochondria-targeted antioxidant therapeutics, Pharmaceuticals (Basel) 4 (3) (2011) 429–456.
[13] T.M. O'connor, J. O'connell, D.I. O'brien, et al., The role of substance P in inflammatory disease, J. Cell Physiol. 201 (2) (2004) 167–180.
[14] H. Wu, C. Guan, X. Qin, et al., Upregulation of substance P receptor expression by calcitonin gene-related peptide, a possible cooperative action of two neuropeptides involved in airway inflammation, Pulm. Pharmacol. Ther. 20 (5) (2007) 513–524.
[15] H.W. Chu, M. Kraft, J.E. Krause, et al., Substance P and its receptor neurokinin 1 expression in asthmatic airways, J. Allergy Clin. Immunol. 106 (4) (2000) 713–722.
[16] Z. Yang, J. Zhuang, L. Zhao, et al., Roles of Bronchopulmonary C-fibers in airway

Hyperresponsiveness and airway remodeling induced by house dust mite, Respir. Res. 18 (1) (2017) 199.
[17] G. Hens, U. Raap, J. Vanoirbeek, et al., Selective nasal allergen provocation induces substance P-mediated bronchial hyperresponsiveness, Am. J. Respir. Cell Mol. Biol. 44 (4) (2011) 517–523.
[18] M.S. Steinhoff, B. Von Mentzer, P. Geppetti, et al., Tachykinins and their receptors: contributions to physiological control and the mechanisms of disease, Physiol. Rev. 94 (1) (2014) 265–301.
[19] N. Liu, L.H. Wang, L.L. Guo, et al., Chronic restraint stress inhibits hair growth via substance P mediated by reactive oxygen species in mice, PLoS One 8 (4) (2013) e61574.
[20] J. Springer, D. Pleimes, F.R. Scholz, et al., Substance P mediates AP-1 induction in A549 cells via reactive oxygen species, Regul. Pept. 124 (1–3) (2005) 99–103.
[21] W.E. Ho, C. Cheng, H.Y. Peh, et al., Anti-malarial drug artesunate ameliorates oxidative lung damage in experimental allergic asthma, Free Radic Biol. Med. 53 (3) (2012) 498–507.
[22] D. Malhotra, E. Portales-Casamar, A. Singh, et al., Global mapping of binding sites for Nrf2 identifies novel targets in cell survival response through ChIP-Seq profiling and network analysis, Nucleic Acids Res. 38 (17) (2010) 5718–5734.
[23] T. Dou, M. Yan, X. Wang, et al., Nrf2/ARE pathway involved in oxidative stress induced by paraquat in human neural progenitor cells, Oxid Med. Cell Longev. 2016 (2016) 8923860.
[24] J.F. Ndisang, A. Jadhav, The heme oxygenase system attenuates pancreatic lesions and improves insulin sensitivity and glucose metabolism in deoxycorticosterone acetate hypertension, Am. J. Physiol. Regul. Integr. Comp. Physiol. 298 (1) (2010) R211–223.
[25] M.P. Seldon, G. Silva, N. Pejanovic, et al., Heme oxygenase-1 inhibits the expression of adhesion molecules associated with endothelial cell activation via inhibition of NF-kappaB RelA phosphorylation at serine 276, J. Immunol. 179 (11) (2007) 7840–7851.
[26] Y. Naito, T. Takagi, Y. Higashimura, Heme oxygenase-1 and anti-inflammatory M2 macrophages, Arch. Biochem. Biophys. 564 (2014) 83–88.
[27] N.G. Abraham, A. Kappas, Pharmacological and clinical aspects of heme oxygenase, Pharmacol. Rev. 60 (1) (2008) 79–127.
[28] K. Kuribayashi, S. Iida, Y. Nakajima, et al., Suppression of heme oxygenase-1 activity reduces airway hyperresponsiveness and inflammation in a mouse model of asthma, J. Asthma 52 (7) (2015) 662–668.
[29] M.R. De Oliveira, G. Da Costa Ferreira, F.B. Brasil, et al., Pinocembrin suppresses H2O2-induced mitochondrial dysfunction by a mechanism dependent on the Nrf2/HO-1 axis in SH-SY5Y cells, Mol. Neurobiol. 55 (2) (2018) 989–1003.
[30] G.M. Walsh, Tralokinumab, an anti-IL-13 mAb for the potential treatment of asthma and COPD, Curr. Opin. Investig. Drugs 11 (11) (2010) 1305–1312.
[31] Man Jia, Xiaoyi Yan, Xinyu Jiang, et al., Ezrin, a membrane cytoskeleton cross linker protein, as a marker of epithelial damage in asthma, Am. J. Respir. Crit. Care Med. 199 (4) (2019) 496–507.
[32] J.J. Lemasters, Selective mitochondrial autophagy, or mitophagy, as a targeted defense against oxidative stress, mitochondrial dysfunction, and aging, Rejuvenation Res. 8 (1) (2005) 3–5.
[33] J. Ohtake, S. Kaneumi, M. Tanino, et al., Neuropeptide signaling through neurokinin-1 and neurokinin-2 receptors augments antigen presentation by human dendritic cells, J. Allergy Clin. Immunol. 136 (6) (2015) 1690–1694.
[34] I. Boldogh, A. Bacsi, B.K. Choudhury, et al., ROS generated by pollen NADPH oxidase provide a signal that augments antigen-induced allergic airway inflammation, J. Clin. Invest. 115 (8) (2005) 2169–2179.
[35] M.R. De Oliveira, F.R. Jardim, Cocaine and mitochondria-related signaling in the brain: A mechanistic view and future directions, Neurochem. Int. 92 (2016) 58–66.
[36] M.R. De Oliveira, Fluoxetine and the mitochondria: A review of the toxicological aspects, Toxicol. Lett. 258 (2016) 185–191.
[37] M.R. De Oliveira, Vitamin A and retinoids as mitochondrial toxicants, Oxid. Med. Cell Longev. 2015 (2015) 140267.
[38] C.L. Quinlan, I.V. Perevoshchikova, M. Hey-Mogensen, et al., Sites of reactive oxygen species generation by mitochondria oxidizing different substrates, Redox Biol, 1 (2013) 304–312.